



ELSEVIER

Geomorphology 37 (2001) 201–223

GEOMORPHOLOGY

www.elsevier.nl/locate/geomorph

# The geomorphology of planetary calderas

Peter J. Mouginis-Mark\*, Scott K. Rowland

*Hawaii Institute Geophysics and Planetology and Hawaii Center of Volcanology, School of Ocean and Earth Science and Technology, University of Hawaii, Honolulu, HI 96822, USA*

Received 1 January 1994; received in revised form 1 July 1996; accepted 14 January 1999

## Abstract

Satellite-derived observations of the geomorphology of calderas on Earth, Mars and Venus can be used to learn more about shield volcanoes. Examples of terrestrial basaltic volcanoes from the Galapagos Islands, Hawaii, and the Comoro Islands show how these volcanoes contrast with examples found on Mars and Venus. Caldera structure, degree of infilling, and the location of vents on the flanks are used to interpret each volcano's recent history. The geometry of the caldera floor can be used to infer some of the characteristics of the magma storage system, and the orientation of the deep magma conduits. The formation of benches within the caldera and the effects of the caldera on the distribution of flank eruptions are considered, and it is evident that most calderas on the planets are/were dynamic features. Presently, deep calderas, with evidence of overflowing lavas and ponded lavas high in the caldera wall, show that these calderas were once shallow. Similarly, shallow calderas filled with ponded lavas are evidence that they were once deeper. It is probably a mistake, therefore, to place great significance on caldera depth with regard to the position, shape, or size of subsurface plumbing. © 2001 Elsevier Science B.V. All rights reserved.

*Keywords:* Geomorphology; Planetary calderas; Volcano

## 1. Introduction

Some of the most impressive features revealed by three decades of planetary exploration are the giant volcanoes of Mars (Fig. 1) and Venus. Observations by the Mariner 9, Viking Orbiter 1 and 2, Pioneer Venus, Venera 15 and 16, and Magellan spacecraft have shown that these extra-terrestrial volcanoes can be up to an order of magnitude higher than their counterparts on Earth, and can display lava flow fields that extend for hundreds of kilometers from

their summit regions (Carr, 1973; Carr et al., 1977; Wilson and Head, 1983; Ivanov and Basilevsky, 1990; Head et al., 1992; Senske et al., 1992). In many cases, martian and venusian volcanoes also possess large calderas at their summits that are reminiscent of the calderas found on basaltic shield volcanoes on Earth.

Calderas have formed on all types of terrestrial volcanoes, and a number of attempts have been made to classify them based on their structure and morphology (e.g., Macdonald, 1972; Williams and McBirney, 1979; Francis, 1993), to which the reader is referred for the basic volcanological nomenclature. The vast majority of magmas on Mars and Venus are believed to be basaltic in composition (cf., Basaltic

\* Corresponding author.

E-mail address: pmm@pgd.hawaii.edu (P.J. Mouginis-Mark).

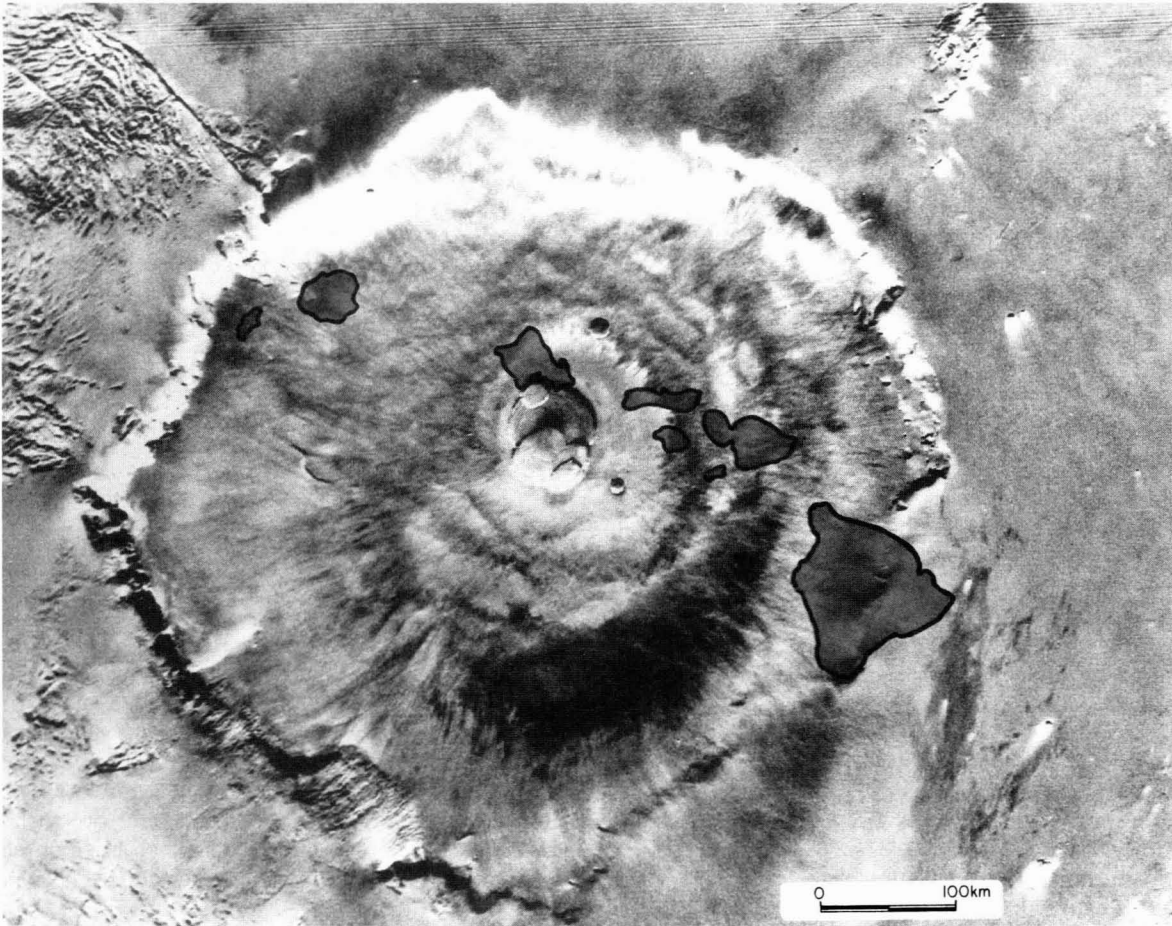


Fig. 1. Viking Orbiter image of Olympus Mons, Mars ( $18^{\circ}\text{N}$ ,  $132^{\circ}\text{W}$ ) with the eight largest Hawaiian Islands superimposed at the same scale to show the relative sizes of the volcanoes. Mauna Loa volcano is located on the Big Island of Hawaii, which is the island at the lower right in this view. Not apparent in this nadir view is the height of Olympus Mons, which rises nearly 27 km above the surrounding plains (far higher than the 8.6 km that Mauna Loa rises from the ocean floor). Viking Orbiter frame 646A28 (724 m/pixel).

Volcanism Study Project, 1981; Francis, 1993), and for this reason our paper considers landforms that are typically associated with basaltic volcanoes on Earth. By definition, terrestrial calderas are depressions  $> 1$  km across that form by gravitational collapse into an evacuated or partially evacuated magma storage complex (or “magma chamber”). This definition differentiates calderas from pit craters, which are smaller ( $< 1$  km diameter) and are formed by collapse into a deep rift zone magma conduit (Walker, 1988), or by shallow explosions generated by rising magma (Macdonald, 1972). On the other planets, where the size of volcanic features is larger (e.g., collapse pits

may be several kilometers in diameter), we propose here that a more convenient definition of a caldera is that the collapse depression has a diameter greater than 10 km.

Through a study of the morphology and structure of their summit areas and calderas, it is possible to learn an appreciable amount about volcano evolution on the planets (Mouginiis-Mark, 1981; Wood, 1984). In certain instances, Viking Orbiter (Mars) and Magellan (Venus) data can provide a clearer picture of the episodes of caldera collapse than is contained within the terrestrial geologic record. This process on Earth, for example, is often masked or destroyed by

subsequent erosion and/or eruptions. By using spaceborne instruments such as the Landsat Thematic Mapper (TM) and the SPOT panchromatic sensor, it is now easier to study the geomorphology of many calderas on Earth that have until now been rarely investigated because of their remote locations. Space remote sensing allows many of the same methodologies of planetary geomorphology to be applied to infrequently studied terrestrial calderas, and provides valuable comparative information. However informative images of these volcanoes are, we nevertheless note that in order to gain a complete understanding of the nature of the basalt volcanism associated with caldera formation and volcano evolution, a comprehensive field, chemical, seismic, deformational, and surface mapping campaign is needed. For extra-terrestrial volcanoes (as well as many terrestrial examples), only surface mapping is possible at the present time, although gravity data for

Mars and Venus permit regional (100–200 km resolution) geophysical knowledge to be gained for the larger volcanoes (Janle and Ropers, 1983; Grimm and Phillips, 1992).

On Earth, knowledge of the spatial distribution of vents and the relative volumes of lava that were erupted provides information on the location and size of magma plumbing systems (Macdonald et al., 1983), the formation of preferred orientations for intrusions (i.e., rift zones), and the significance of edifice and regional stress fields (Nakamura, 1977, 1982; Chadwick and Howard, 1991; Munro, 1992; Rowland and Munro, 1992). All of these factors are relevant to the study of the collapse events associated with calderas on Earth (Decker, 1987), and they are relevant to the other planets as well. The temporal distribution of eruptive vents is equally important as it permits an understanding of the evolution and development of the magma supply system. For ex-

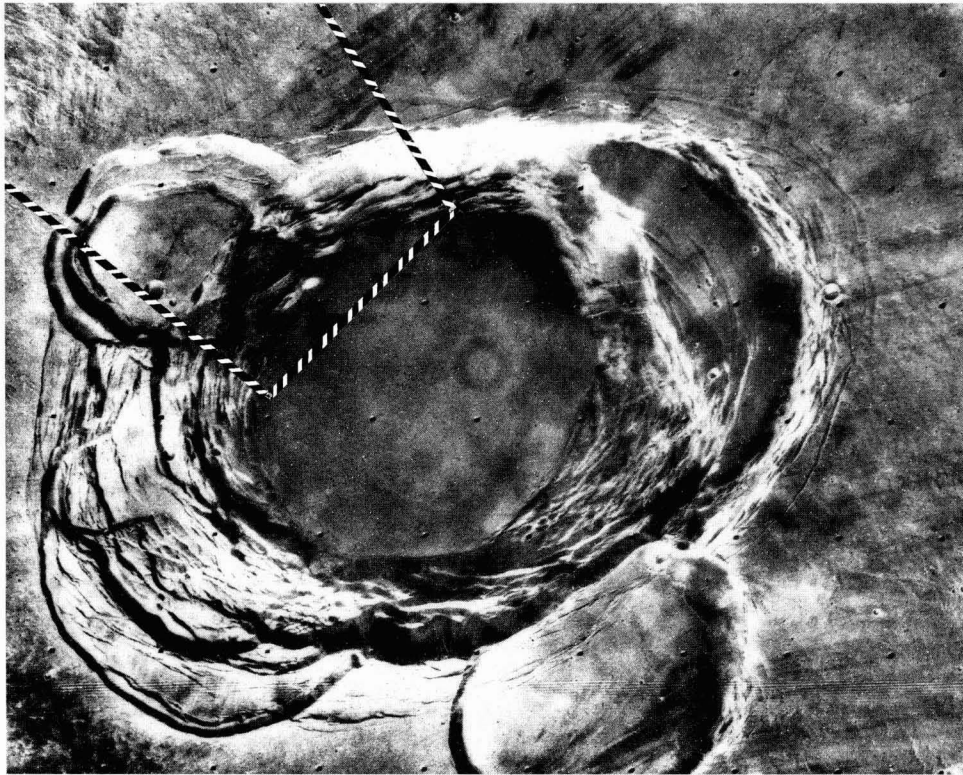


Fig. 2. View of the summit caldera of Ascræus Mons volcano, Mars ( $11^{\circ}\text{N}$ ,  $105^{\circ}\text{W}$ ), showing the multiple collapse pits. Location of Fig. 6 is shown by the outlined area at top left. Notice that the youngest (central) collapse event produced the largest segment of the caldera ( $40 \times 38$  km across), which is opposite from the Olympus Mons caldera (Fig. 1). Viking Orbiter frame 90A50 (63 m/pixel).

ample, changes in location of vent areas as a function of time can be seen on Mauna Loa, Hawaii (Lipman, 1980a,b; Lockwood and Lipman, 1987) and Wolf volcano, Galapagos Islands (Munro et al., 1991).

Four main questions occur that imaging from spacecraft can address for basaltic calderas on any planet.

(1) What is the chain of events that led to the present morphology of a caldera (can the episodes of infilling and collapse be identified), and what is the present state?

(2) What is the nature of magma storage beneath the summit of the volcano, and how does the pattern of collapse features at the surface provide an insight into this subsurface structure?

(3) Based on the distribution of extra-caldera collapse features (pit craters) and flank vents, what is the orientation of deep magma conduits emanating

from the central magma storage complex? Does evidence exist for the development of linear lines of collapse pits and vent concentrations that suggest rift zones? Can the stress field orientations of the edifice and/or region be determined and if so, what are they?

(4) How does the presence and morphology of a caldera affect the location and/or orientation of eruptive fissures on the volcano?

The objective of this paper is, therefore, to describe how the satellite-derived observations of the geomorphology of calderas on Earth, Mars and Venus can be used to learn more about basaltic volcanoes. Through the use examples from the Galapagos Islands, Hawaii, and the Comoro Islands, we show how these volcanoes contrast with examples found on Mars and Venus. Caldera structure, degree of infilling, and the location of vents on the flanks are used to interpret the recent history of each volcano.

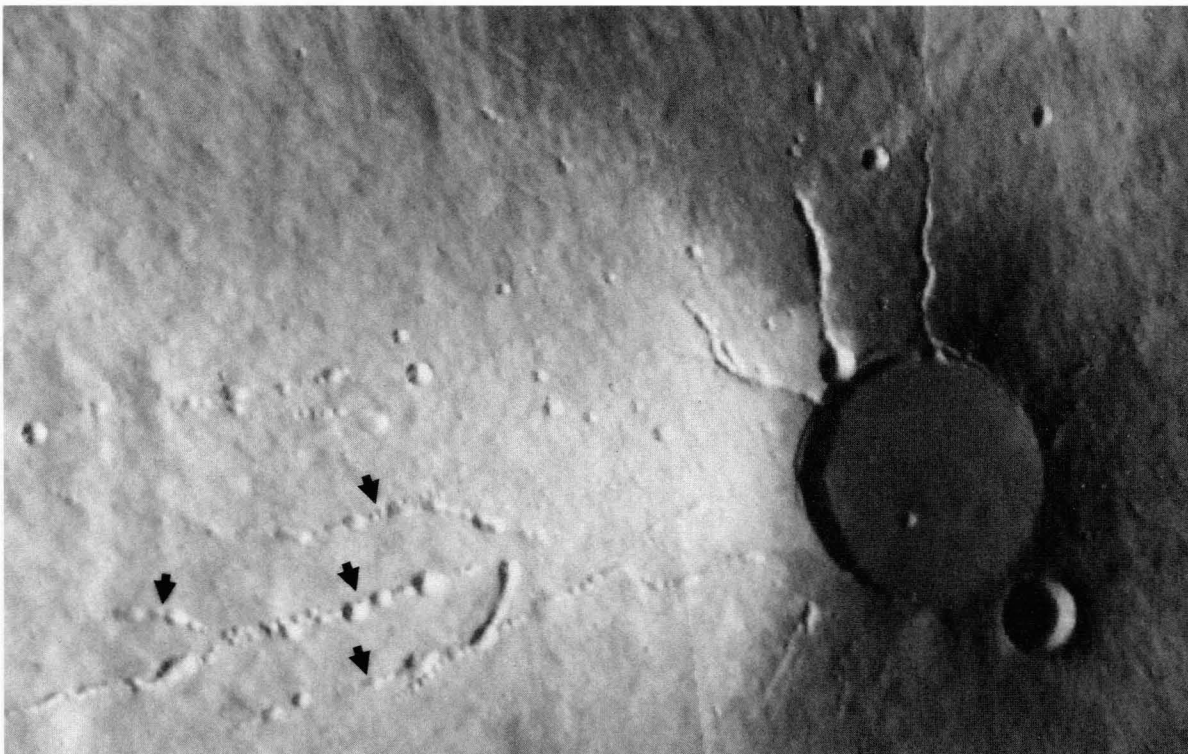


Fig. 3. The summit of Elysium Mons volcano, Mars (25°N, 213°W) has a 10-km diameter caldera, which appears to have formed by a single collapse event. Also visible are several pit chains (arrowed) that probably mark the locations of subsurface magma conduits or lava tubes. Valleys on the north rim are probably lava channels. Viking Orbiter frames 541A42 and 44 (144 m/pixel). Image width is 90 km, with north towards the top.

## 2. The recent history and present state of a caldera

Investigations of the calderas of terrestrial basaltic volcanoes have shown that they typically form incrementally (Decker, 1987). Mapping of Hawaiian volcanoes (Holcomb, 1987; Lockwood and Lipman, 1987) has shown that during the most active period in a basaltic shield's growth, there is no obvious relationship between a caldera and the stage of evolution of these volcanoes. Rather, basaltic calderas are transient, recurring features that can evolve, increase in size, and become infilled without greatly influencing the rate or type of eruption. Here, we consider two aspects of the recent history and present state of calderas: collapse events and infilling.

### 2.1. Collapse

Calderas are often considered to be evidence of catastrophic collapse. On silicic volcanoes, this is a good assumption because specific erupted products can often be correlated with the caldera (e.g., the Taupo volcanic zone in New Zealand; Wilson et al., 1984) and the Quaternary calderas of the Alaska Peninsula (Miller and Smith, 1987). Application of this idea has been a relatively unsuccessful exercise at basaltic volcanoes for two reasons: (1) there have not been many examples of major collapses at basaltic volcanoes in historic time; and (2) those that have occurred have been accompanied by little or no erupted lava (Jaggard, 1947; Macdonald, 1965, 1972;

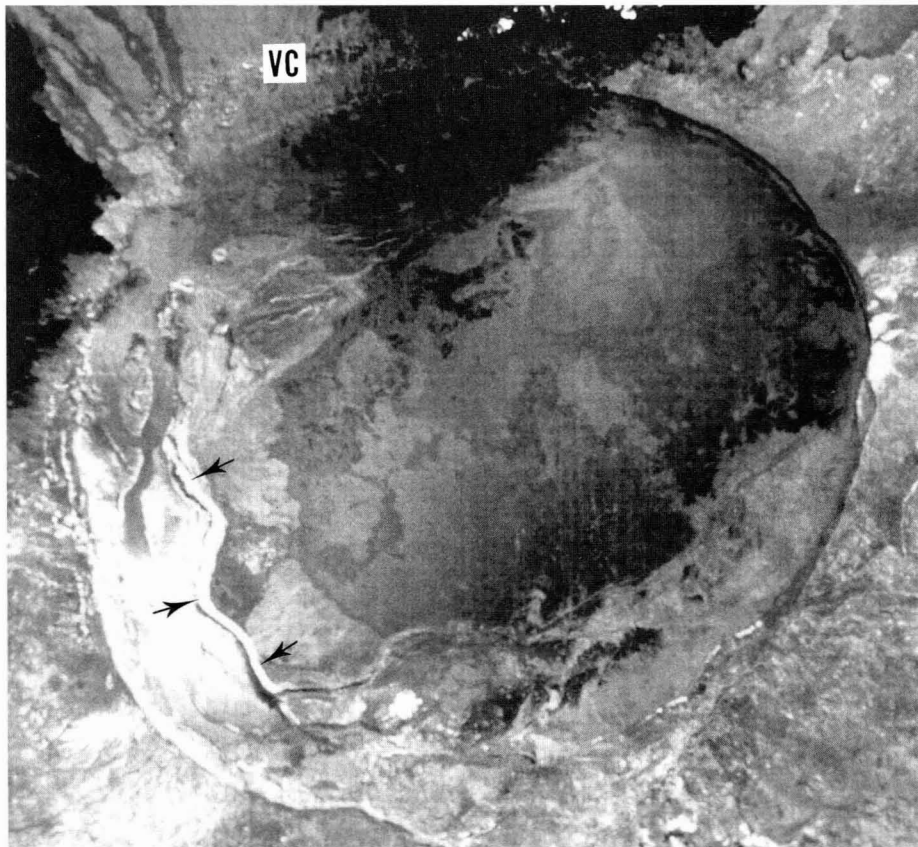


Fig. 4. SPOT panchromatic image (10 m/pixel) of the caldera of Sierra Negra volcano, Galapagos Islands. Prominent on the western side of the caldera floor is a sinuous ridge (arrowed) that probably formed during subsidence of the floor. The caldera is  $7.4 \times 9.3$  km in diameter. Volcano Chico (VC) is the site of recent activity from arcuate fissures located on the northern rim. North is to the top of this image. © SPOT Image Corp.

Simkin and Howard, 1970). During the 1924 collapse at Kilauea caldera, seismicity and ground deformation indicated that magma was intruded at least

as far as the subaerial extent of the East Rift Zone at Kapoho, about 45 km from the summit caldera (Jaggard, 1947; Devorak, 1992). In the Galapagos, the



Fig. 5. SPOT panchromatic image (10 m/pixel) image of Mokuaweoweo Caldera on Mauna Loa volcano, Hawaii. The light tones in this image are pahoehoe flows that over spilled the caldera rim about 600 years ago, and indicate that recently the entire caldera was full. Dark tone flows are the younger a'a flows. North to top of image. © SPOT Image Corp.

1968 collapse of Fernandina was perhaps associated with magma that was intruded and not erupted, or maybe lava erupted undetected under water (Simkin and Howard, 1970). Another possibility is that caldera collapse is not due to a single event, but rather the accumulated strain of numerous magma

excursions that were not fully replenished by magma from the mantle. The eruption of a small volume of lava at Fernandina in 1968 might have only been the trigger that released accumulated strain from numerous earlier eruptions. Certainly, there were previous eruptions at Fernandina of much larger volume (for

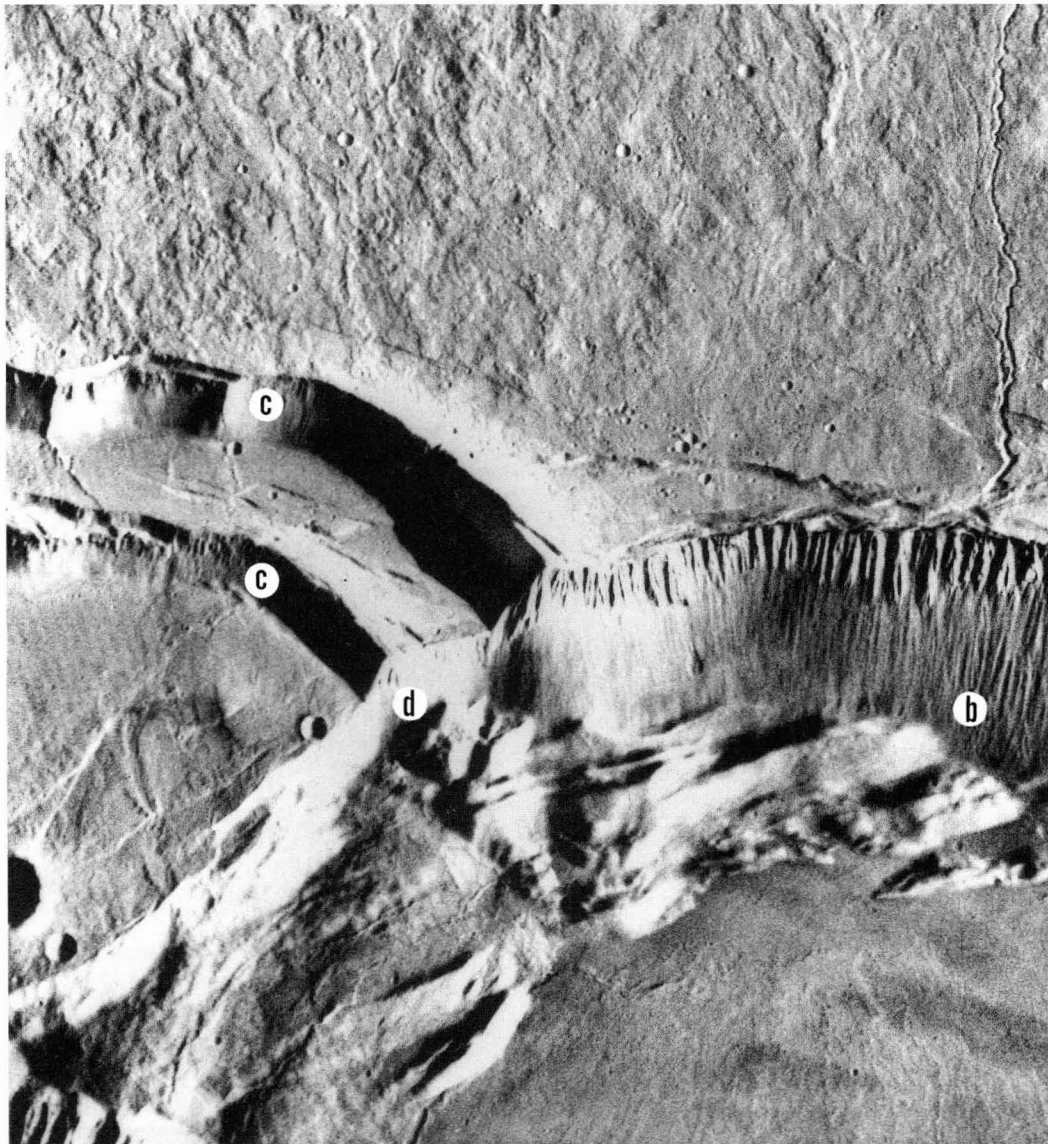


Fig. 6. High resolution image of the southern rim of Ascræus Mons caldera, Mars. See Fig. 2 for location. Notice the fluting close to the rim, the extensive talus deposits, multiple levels to the caldera floor, and the beheaded lava flows. The areas labeled *b*, *c*, and *d* are the locations where we expect that higher resolution data comparable to those shown in Fig. 18b–d would reveal similar details of the structure of this caldera. Viking Orbiter image 401B20 (22 m/pixel).

example, that of 1958; Richards, 1960; Rowland and Munro 1992) that were not accompanied by caldera collapse. Indeed, large eruptions at most terrestrial basaltic volcanoes have been unaccompanied by significant collapse. The magnitude of collapse events on Mars would have been immense, had the caldera formation been the result of a single eruption. For example, the volume of individual collapse features on the Martian volcano Ascraeus Mons (Fig. 2) can be as great as  $3760 \text{ km}^3$ , and on Olympus Mons (Mars) this volume can be as great as  $5145 \text{ km}^3$  (Mouginiis-Mark, 1981). Such collapse events were more likely incremental, and associated with the collective effects of many tens to hundreds of eruptions or intrusions, based on the volumes of lava flows seen on the flanks of these volcanoes (Mouginiis-Mark, 1981).

The common result of a collapse event is a funnel-shaped talus-lined depression, rather than a flat floor that has dropped like a piston. Examples of this type of depression include the 1968 collapse of Fernandina (Simkin and Howard, 1970), the 1924 collapse of Halemaumau in Kilauea (Jaggard, 1947), and the 1918 enlargement of the central vent in the Karthala caldera (Strong and Jaquot, 1971; Upton et al., 1974). Later infilling by lava usually buries the talus leaving a flat floor. Caldera benches are most commonly the result of earlier levels of ponded lava left behind by smaller-scale collapse, rather than blocks that have dropped intact from higher levels of the caldera wall (McBirney and Williams, 1969; Simkin and Howard, 1970). It is likely that the almost circular 10 km diameter caldera of Elysium Mons on Mars (Fig. 3) formed by a single collapse,

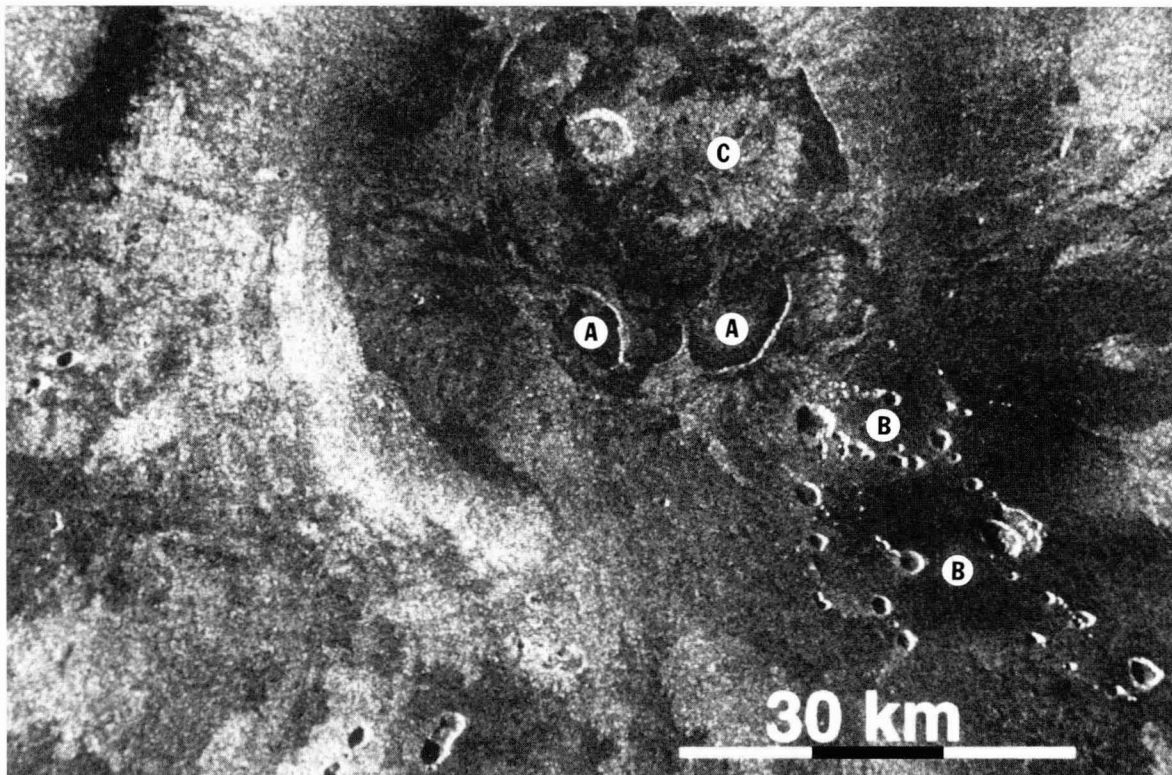


Fig. 7. The summit area of Maat Mons, Venus, shows multiple collapse pits at the summit (A) and on the high flanks (B), indicating multiple storage reservoirs for the near-surface magma. Also indicated is a small radar-bright lava flow (C), which shows that there have been at least two episodes of activity since the caldera formed (i.e., the original resurfacing event and the formation of flow c). Maat Mons is located at  $1^{\circ}\text{N}$ ,  $194^{\circ}\text{E}$ , and has a caldera that is  $31 \times 28 \text{ km}$  in diameter.

because no remnants of separate collapse episodes seen around the rim. In addition, no sign of “caldera benches” occur within the Elysium Mons caldera, and the absence of such features indicates that a single event most likely formed the summit caldera. Non-catastrophic subsidence of a caldera floor covered by infilling flows is believed to account for the morphology of the Olympus Mons caldera, Mars (Mouginis-Mark and Robinson, 1992; Zuber and Mouginis-Mark, 1992), where extensional graben have formed around the perimeter of the caldera floor and pressure ridges formed toward the center. More than 1300 m of elevation difference exists within a single segment of the caldera floor of Olympus Mons, and comparable deformation of the infilled surface has also been identified for Apollinaris Patera, Mars (Robinson et al., 1993). Pavonis

Mons may be a third Martian example of this type of deformation (Mouginis-Mark et al., 1992). A conspicuous ridge in the caldera of Sierra Negra, Galapagos Islands (Fig. 4) may be a good terrestrial example of this post-caldera-flooding deformation (Munro, 1992).

### 2.2. Infilling

The other important observation bearing on the dynamism of basaltic calderas is that they can be either partially or wholly infilled. Detailed mapping at Mauna Loa and Kilauea has shown that during the past 1000 years both calderas have been filled to overflowing (Macdonald, 1972; Lockwood and Lipman, 1987; Holcomb, 1987). This is evident on Mauna Loa where numerous flows southeast of the

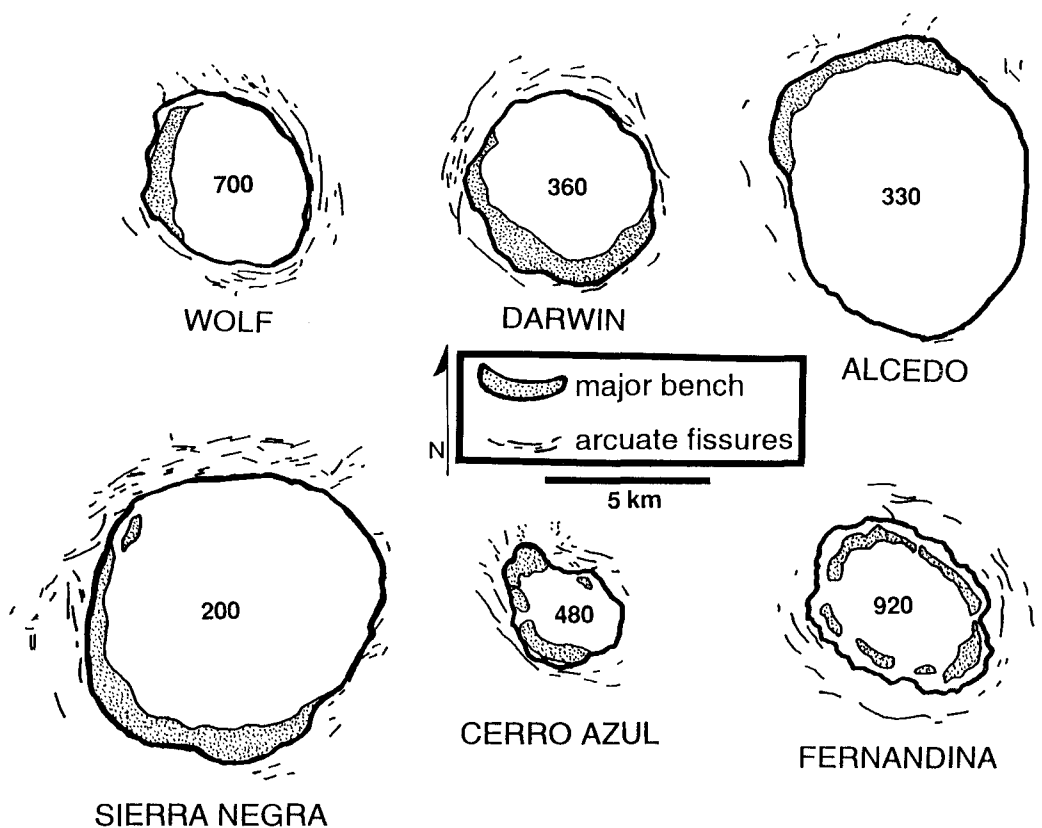


Fig. 8. Comparison of the six major calderas in the Western Galapagos Islands, showing caldera outlines, locations of major intra-caldera benches, and the distribution of recently active arcuate fissures on the upper outer flanks. Numbers give the average depth of each caldera in meters. Prepared from maps in Munro (1992).

caldera are truncated by the present caldera wall (Fig. 5). The most obvious of these are large a'a flows, however, the majority of lava erupted during the period of overflowing was tube-fed pahoehoe (Lockwood and Lipman, 1987). Much of the surface of Kilauea southwest of the caldera is comprised of similar tube-fed pahoehoe, and can also be related to an overflowing caldera (Holcomb, 1987). This same situation may also apply to Mars and Venus in certain instances. For example, it has been proposed that flows over-spilled the southern rim of the Ascraeus Mons (Mars) caldera (Fig. 6) before the latest episodes of collapse took place (Mouginis-Mark, 1981), and radar-bright flows that are cut by the eastern caldera rim of Maat Mons on Venus (Fig. 7) may indicate a similar process.

The six active shield volcanoes on the islands of Isabela and Fernandina in the Galapagos Archipelago are notable for their large calderas, especially when

compared to the size of the volcanoes themselves (Nordlie, 1973), and provide some fine examples of the diverse morphology of calderas on basaltic volcanoes (Fig. 8). The Galapagos calderas average  $\sim 6$  km in diameter but vary greatly in depth from  $\sim 200$  m at Sierra Negra to  $\sim 920$  m at Fernandina. The Galapagos calderas are likely to have been as dynamic as Hawaiian calderas, and indeed the deeper Galapagos calderas show evidence of once being shallower (e.g., ponded lava flows exposed high in the walls; Chadwick et al., 1991), and the shallow ones show evidence of having once been deeper (presently filled by ponded lava flows). The lavas that infill calderas are usually thick and flat-lying, making them easy to distinguish from flank flows when they are exposed in section.

Some martian calderas are only a few hundred meters deep (e.g., Alba Patera; Fig. 9), while others are very deep (e.g., Tharsis Tholus has a caldera  $> 4$



Fig. 9. Alba Patera, Mars ( $40^{\circ}\text{N}$ ,  $109^{\circ}\text{W}$ ) has two discrete summit calderas, of which this one is the only one that has a complete rim crest. The wrinkle ridges on the caldera floor, and the lack of benches around the rim, both suggest that this caldera has probably been partially infilled after the initial collapse. Notice the similarity between the morphology of this caldera and that of Sierra Negra (Fig. 4). The width of the caldera is  $45 \times 65$  km. Mosaic of Viking Orbiter images 253S13 to 16 (73 m/pixel). North to top of image.

km deep; Robinson, 1994), and this may reflect different degrees of infilling after collapse. The wrinkle ridges to the north of the existing caldera of Pavonis Mons (Zimelman and Edgett, 1992) may indicate a larger, now entirely infilled caldera once existed. Most preserved calderas on Venus are also relatively shallow. Although the Magellan altimetric data have insufficient spatial resolution to determine confidently absolute depths, in a qualitative sense, these calderas appear to be shallower based on the length of the radar shadows. The Venus calderas (such as Sacajawea, which is  $150 \times 105$  km in diameter) appear to have flat floors and are talus-free, so we infer that they have been partially infilled by ponded lava. Within the caldera of Maat Mons (Fig. 7), the generally radar-dark floor appears to have been partially buried by small ( $\sim 10 \times 15$  km) flows that originated from two of the smaller pits within the caldera. There is little evidence in the Magellan

data that sagging or subsidence of the summits took place following the infilling of the calderas on Venus.

### 3. The central magma storage system

Most calderas have complex morphologies that indicate that they are composed of multiple rather than single collapse features (Strong and Jaquot, 1971; Macdonald, 1972). A few notable examples are Mauna Loa, Karthala (Grand Comoro Island; Fig. 10), Olympus Mons (Mars), and Cerro Azul (Galapagos Islands). The separate collapse features are usually at different depths within a caldera complex, and may be obvious near-circular structures that are joined barely to each other (e.g., Mauna Loa), or may merely be large scallops in the outline of the caldera (e.g., Kilauea). In all these examples, the individual features may have collapsed numerous

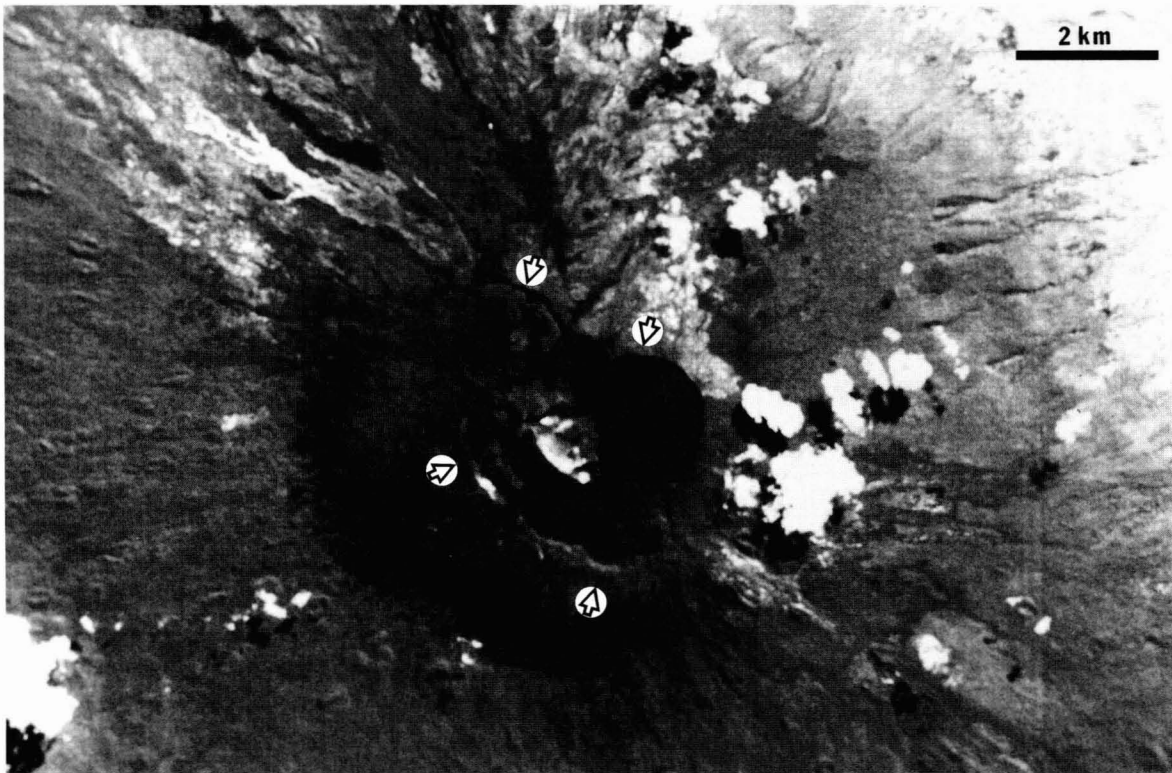


Fig. 10. SPOT color Band 2 image (20 m/pixel) image of Karthala volcano, Grand Comoro Islands ( $11.75^{\circ}\text{S}$ ,  $43.38^{\circ}\text{E}$ ). The rim crest of the caldera is indicated by the arrows. See also Fig. 11 for the reconstructed chronology of collapse events for the volcano. North is towards the top. © SPOT Image Corp.

times, and may have formed separately from each other, only to be combined by infilling of later intra-caldera lavas. Subsequent collapse of nearby areas may strand portions of these collapse features at levels above the main caldera (e.g., Fernandina and Karthala volcanoes) to form intra-caldera benches. Examples from Mars (e.g., Alba Patera and the complex within Syrtis Major) show that it is also possible for physically separate calderas to form on the same volcano (Schaber, 1982; Mougini-Mark et al., 1988). The 4 million-year-old Kauai volcano (Hawaii) also apparently developed two calderas (Macdonald, 1972).

Fiske and Kinoshita (1969) were the first to determine that the magma storage complex of Kilauea is comprised of multiple storage zones rather than a single void. They followed the detailed deformation history of the volcano during the episode of inflation

prior to an eruption, and then during the subsequent deflation episode. Fiske and Kinoshita found that the center of deformation migrated during these episodes and that the order of migration during the deflation was not the reverse of that during the inflation. Their conclusion was that the magma storage system consisted of a plexus of interconnected voids that could fill and empty one after another in response to either rising or falling magma pressure.

Although the Kilauea events studied by Fiske and Kinoshita (1969) produced no collapse features (the volumes involved were small), we interpret the presence of multiple collapse features on basaltic calderas elsewhere to be evidence of the same type of subsurface plexus of storage voids. As noted above, basaltic calderas are very dynamic structures, and undergo numerous collapse and infilling episodes during the active life of a volcano. A good example of this is

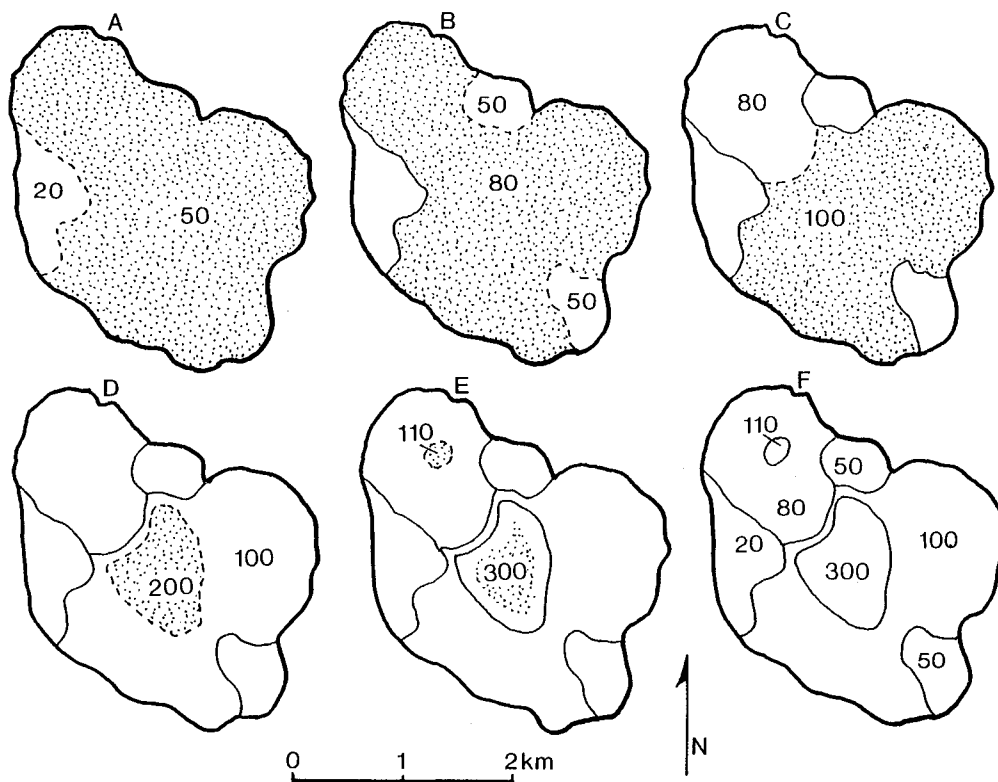


Fig. 11. Stages in the development of the present configuration of the Karthala caldera, with numbers indicating the depth (in meters) below the main caldera rim. (A to E) Each event involves the collapse and infilling of a section of caldera (stippled) to a new depth, and forming a new scarp (dashed). The last event (E) occurred in 1918 and involved the deepening of the central pit and the formation of a smaller (new) pit in the north. (F) shows the present state of the caldera.

the evolution of the caldera of Karthala volcano, for which the sequence of events has been reconstructed (Fig. 11). Furthermore, the terrestrial examples can be used to imply that certain planetary volcanoes also once possessed complicated storage reservoirs. The numerous small ( $\sim 10$  km diameter) overlapping collapse pits at the summit of Sif Mons, Venus (Senske et al., 1992) probably indicate that multiple collapses took place over an extended time period, in a manner comparable to the evolution of the caldera of Olympus Mons and other volcanoes on Mars (Mouginis-Mark et al., 1992). In some instances, such as Asraeus Mons (Mars), the most recent

sequence of collapse involved progressively larger volumes of material, while at Olympus Mons the opposite trend has been identified (Mouginis-Mark, 1981).

A relationship probably exists between the size of this magma storage system in a volcano and the diameter of the caldera (Koyanagi et al., 1972). Most often this storage system is referred to as the “magma chamber”, although as noted above it is probably a series of inter-connected voids (Fiske and Kinoshita, 1969; Ryan, 1988; Walker, 1988; Delaney et al., 1990). The exact size and geometry of the storage system is complicated by the fact that it is unlikely

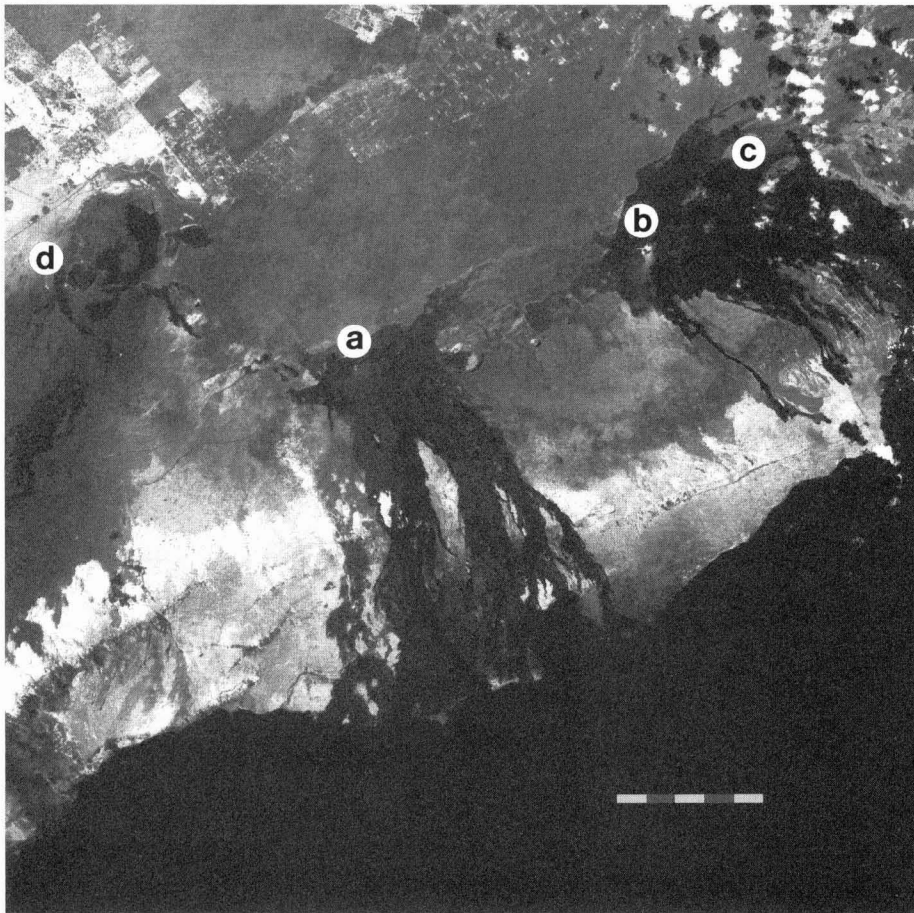


Fig. 12. The East Rift Zone of Kilauea volcano, Hawaii, is a classic example of a chain of collapse pits over-lying a subsurface magma conduit. In this instance, young lava flows have been erupted from the Mauna Ulu (a), Pu'u 'O'o (b), and Kupaianaha (c) vents, which are  $\sim 10$ ,  $\sim 20$  and  $\sim 23$  km down rift from Halemaumau pit crater (d) in the summit caldera of Kilauea. Landsat Thematic Mapper image (30 m/pixel) obtained in October 1991. Scale bar is 5 km. North to top of image.

that a reservoir will be completely emptied during an eruption. Numerical models (e.g., Zuber and Mouginis-Mark, 1992), however, indicate that a relationship may exist between the reservoir depth, the distribution of tectonic features (wrinkle ridges that have formed by compression and graben) and the topography of the caldera. If this relationship is true, identifying even the most general characteristics of the size and depth of the magma chamber for extraterrestrial volcanoes may have importance in interpreting volcanic processes in the Solar System such as heat flow, crustal density, volatile content of the

magma, and crustal thickness. In the case of Venus, for example, the development of relatively deep neutral buoyancy zones (one which lies within the crust rather than the edifice) may encourage large magma reservoirs to form with widely distributed pathways to the surface (Head and Wilson, 1992). This situation should promote the formation of broad low shields with multiple source vents, but in places where high volcanoes do form, the displacement of larger volumes of magma (compared to terrestrial volcanoes) could result in larger calderas forming on Venus than on Earth.



Fig. 13. Numerous collapse pits and chains (arrowed) on the northern rim of the caldera of Arsia Mons volcano on Mars (10°S, 120°W). These may mark the surface expression of subsurface magma conduits that are comparable to the rift zone on Kilauea volcano (Fig. 12). Notice also the three prominent elongate fissures (f) with ramparts around their rims on the caldera floor that are parallel to the collapse pits, suggesting a tectonic influence. Viking Orbiter image 422A35 (40 m/pixel). Image width is 40 km and north is towards top.

#### 4. Distribution of flank magma conduits

There are a number of surface features that are often seen close to calderas that provide evidence for the distribution and concentration of magma conduits within the flanks of the volcano. Extra-caldera pit craters are common on Hawaiian shield volcanoes as well as on some extra-terrestrial examples. In most cases, they are often distributed along linear zones which, in the Hawaiian examples (e.g., Kilauea; Fig. 12), are the rift zones (also defined by concentrations of subparallel vents, graben, and broad topographic highs; e.g., Macdonald et al., 1983). Pit craters occasionally form at the site of prolonged flank activity (e.g., those at Pu'u 'O'o and Mauna Ulu; Swanson et al., 1979; Tilling et al., 1987; Heliker and Wright 1991). However, most pit craters are not associated with particular eruptions, although eruptions can take place within them, nearby, or apparently without being affected by their presence (Macdonald, 1972).

Seismic data indicate the presence of a magma conduit 2.5 to 3.5 km deep underlying the East Rift Zone of Kilauea (Klein et al., 1987), and it is this conduit that feeds magma to vents along the rift. Walker (1988) presented a model of pit crater formation over such a conduit, which indicates that pit craters form by the upward stopping of a void formed over the major conduit. The importance of Walker's model is that there needs to be a long-lived void into which the material can fall and be carried away, and the best interpretation is a major magma conduit. This model fits well with the Devil's Throat pit crater on the East Rift Zone of Kilauea, which when first observed by westerners consisted of a cupola-like structure with a small opening into a much larger void (Jaggard, 1947, p. 80); the last lavas had yet to fall in. More recently, these lavas have fallen in and Devil's Throat has evolved into the more typical cylindrical form of a pit crater. The Galapagos volcanoes display slight concentrations of radial flank



Fig. 14. The summit area of Sif Mons, Venus (22°N, 352°E) shows numerous pit craters and crater chains. Also visible in this Magellan radar image is the distribution of radar-dark flows on the western outer flanks. These may indicate smoother lava flow textures, perhaps comparable to terrestrial pahoehoe flows. The caldera is 40 km in diameter. North to top of image.

vents (McBirney and Williams, 1969; Chadwick and Howard, 1991); however, these do not appear to be rift zones in the sense of the Hawaiian cases.

Fine examples of lines of pit craters are also found on the northern flank of Elysium Mons, Mars (Fig. 3). Three valleys cut the northern caldera wall,



Fig. 15. The asymmetric distribution of lava flows on the flanks of Cerro Azul volcano, Galapagos Islands is evident in this SPOT panchromatic image (10 m/pixel). Almost all of the youngest flows from arcuate fissures are located on the northern flank. This may be relevant to any consideration of the effects of intra-caldera structure on the distribution of magma pathways within the volcano, because there is a large intra-caldera bench on the southern wall (i.e., the bench may preclude dike propagation in the vicinity on the southern caldera rim). Scale bar is 5 km. North is towards the top of the image. © SPOT Image Corp.

and extend  $\sim 10$  km down slope, at which point they continue down slope as lines of pit craters. No raised rims can be seen around any of these pits, so that they are interpreted to have formed by collapse of a lava tube (Malin, 1977), however, it is also possible that they are the surface expression of deeper magma conduits (rift zones). Aligned collapse pits can also be found on the northern rim of the Arsia Mons (Mars) caldera (Fig. 13) and these may also mark the location of a subsurface magma conduit. On Venus, Sif Mons (Fig. 14) and Maat Mons (Fig. 7) have distinct chains of pits  $\sim 3$  km across, which radiate from the caldera rim for distances up to  $\sim 40$  km. In a few cases, the pits on these volcanoes have coalesced into fissures that are comparable to the Elysium Mons examples. There does not appear to be much of a preferred orientation for these chains

on Venus, giving the impression that if the depressions are pit craters that formed over major magma conduits. These conduits are more numerous than on Hawaii rift zones and their locations are not as tightly localized as are those feeding Hawaiian rift zones.

##### 5. The effect of the caldera on vent orientation and distribution

Flank vents can also form parallel (rather than perpendicular) to the contours. These have often been termed “circumferential” vents and they are best displayed on the Galapagos shields (McBirney and Williams, 1969), however, Munro (1992) suggested that such vents be termed “arcuate” rather

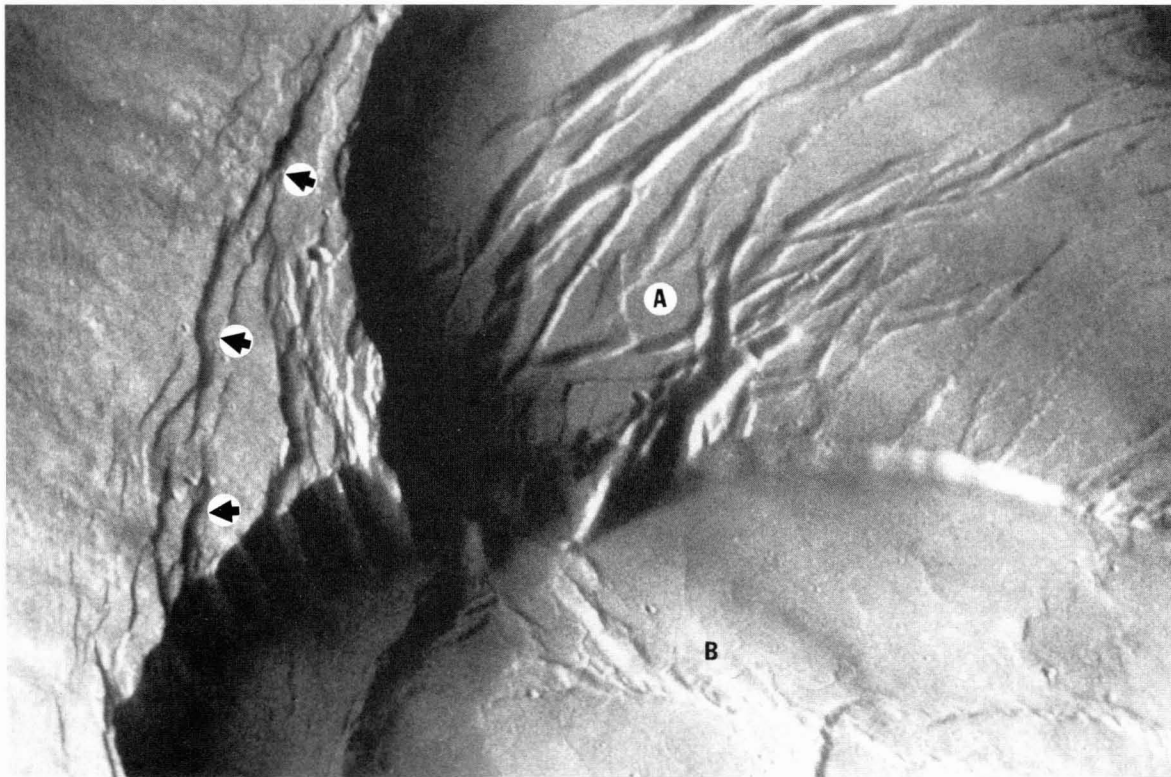


Fig. 16. Oblique view of the western side of the Olympus Mons caldera, Mars. Notice the different degrees of tectonic deformation on the caldera floor, with older segments (A) displaying graben while the younger floor (B) is smooth following a resurfacing event. Fractures (arrowed) on the caldera wall may mark the locations of incipient slump blocks, where future caldera widening might occur. Width of image is  $\sim 25$  km and the height of the main caldera wall is  $\sim 2$  km (Mouginis-Mark and Robinson, 1992). Viking Orbiter image 475S03 (28 m/pixel), with north towards the top left of the image. The illumination is from the left in this view.

than circumferential because none of them extend the entire way around the caldera rim. Fig. 15 shows Cerro Azul volcano, Galapagos, which has a  $4.3 \times 3.2$  km diameter caldera that is  $\sim 480$  m deep. Within the caldera, two major benches and numerous slump blocks occur. As observed by Munro (1992), recent activity at Cerro Azul (and at Volcan Darwin and Sierra Negra), has been limited to arcuate vents that occur along well-defined sectors of the summit plateau. Munro and Rowland (1993) suggest that an unbuttressed caldera wall sets up a radial pattern of sigma-3 in its vicinity, leading to the formation of arcuate vents. An examination of the presence of intra-caldera benches and their proximity to the recently active arcuate vents around the summit areas of the Galapagos volcanoes suggests that they may inhibit near-caldera eruptions by buttressing the walls (Fig. 8).

The west wall of the Olympus Mons caldera (Fig. 16) illustrates dramatically the effect of the caldera on the local minimum stress field (sigma-3). Although no vents can be identified, a distinct pattern of open fractures indicates a very obvious direction of tension that is perpendicular to the caldera wall.

Any dikes that did propagate into this part of the volcano would orient themselves parallel to the caldera wall and become arcuate vents such as those on the Galapagos. Nevertheless, a few complications occur to this model for the martian and terrestrial volcanoes in terms of how the orientation of fissures relates to the stress field. For example, even though the depths of the calderas in the Galapagos vary from 1000 to 100 m, all of the calderas possess arcuate fissures. Even if a caldera is full (or nearly full), enough of a perturbation occurs in the stress field to orient sigma-3 radially in the vicinity of the caldera. An excellent example of this is Sierra Negra (Fig. 4) with a caldera only 110 m deep, where most historic eruptions have occurred from an arcuate fissure system called Volcan Chico (Delaney et al., 1973).

Unfortunately, the resolution of images of Mars and Venus is insufficient to resolve confidently vent locations, although spatter ridges have been identified at Alba Patera, Mars (Cattermole, 1986). Typically for planetary volcanoes, the distribution of lava flows is used to provide evidence of where the vents are located. Some of the best evidence for circumfer-

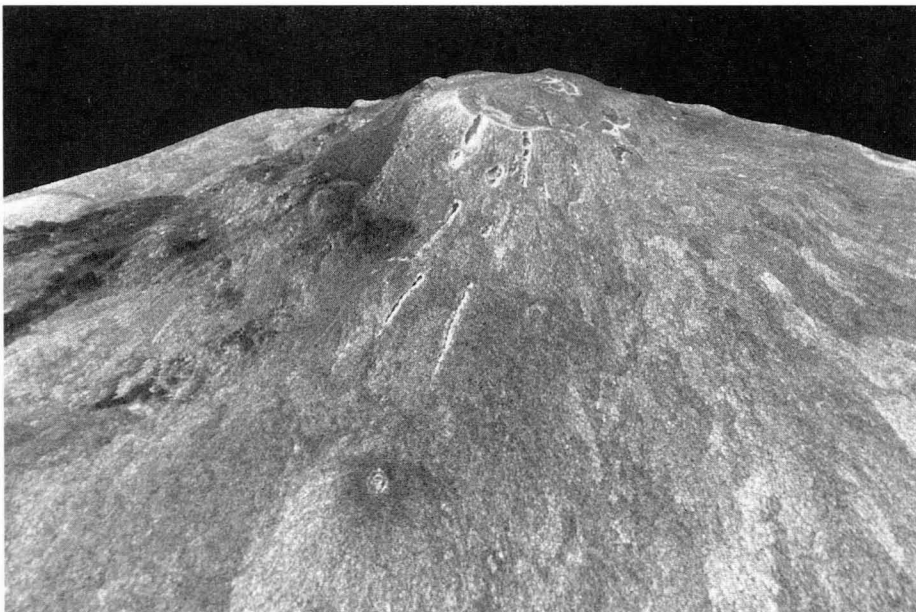


Fig. 17. Computer-generated oblique view of Sif Mons volcano, Venus, as viewed from the southeast. Notice that the radar-dark lava flows identified in Fig. 14 were erupted from vents close to the caldera rim and on the middle flanks. This image has been generated using Magellan altimetric data and is displayed with a  $15 \times$  vertical exaggeration.

ential vents can be seen on Pavonis Mons, where several sinuous rilles originate close to the rim (Zimbelman and Edgett, 1992), on Arsia Mons where young flows originate on the northern part of the caldera rim and flow down the walls towards the floor (Mougini-Mark, 1981), and on the western flank of Alba Patera where young flows emanate from circumferential fractures (Cattermole, 1990). At Sif Mons, Venus (Fig. 17), radar-dark flows are found on the west and southwest flanks at 12 and 70 km from the caldera rim and correspond to vent elevations of 2.5 and 0.9 km above the 6051.84 km mean planetary radius. Numerous small “fans” of radar-bright flows (which are most likely comparable to the high volumetric flow rate eruptions of a’*a* on Earth) are particularly prominent on the eastern flank of Sif Mons (1.9 to 2.0 km elevation) ~ 35 km from the caldera rim, and the lower southern flank of Maat Mons at ~ 5.1 km elevation about 60 km from the rim.

## 6. Discussion and conclusions

Satellite images of calderas and their parent volcanoes enable several aspects of the evolution of a caldera to be determined. The synoptic view of terrestrial (Figs. 5, 10, 12 and 15) and extra-terrestrial (Figs. 1, 7 and 14) volcanoes enables geomorphic features such as benches within the caldera and the geometry of the caldera floor and walls to be used to infer some of the characteristics of the magma storage system, the orientation of the deep magma conduits, and the effects of the caldera on the distribution of flank eruptions. In addition, it is evident that most calderas on the planets are/were dynamic features. Presently, deep calderas with evidence of overflowing lavas and ponded lavas high in the caldera wall show that these calderas were once shallow. Similarly, shallow calderas filled with ponded lavas are evidence that they were once deeper. It is probably a mistake, therefore, to place great significance on caldera depth with regard to the position, shape, or size of subsurface plumbing.

Although the detailed mapping necessary to determine the timing of collapse events at extra-terrestrial volcanoes has not yet been carried out for many volcanoes, evidence for an evolving, dynamic caldera

can still be found. For example, analogies between the high resolution Viking Orbiter views of the summit of Ascræus Mons on Mars (Fig. 6) and the wall of Fernandina caldera in the Galapagos Islands (Fig. 18a) are striking, and it is reasonable to assume that a common process of caldera collapse and infilling was associated with both examples. We can use this similar large-scale morphology to predict the localities on the planetary volcanoes where key field observations (or high-resolution satellite measurements) could be made that would give us new insights into their evolution. For example, were the spatial resolution of the Viking Orbiter data of the same scale as can be achieved from field observations, the types of features on Ascræus Mons that would be sought for include the following.

(1) The degradation of talus slopes, which may give an idea of the relative maturity of each segment of the wall (Fig. 18b).

(2) The relative thickness of lava flows in the wall units (Fig. 18c). Particularly for the thicker flows, which can be inferred to have ponded within an earlier caldera, it is possible to calculate an approximate volume for each eruption based on flow thickness and caldera area.

(3) If there are major discontinuities within the sequence of flows in the wall (Fig. 18d), this is a clear indication that earlier episodes of caldera flooding and collapse have taken place that might not be visible in nadir-viewing satellite images.

The above observations should be taken as a generic set of geomorphic data that could be collected for calderas on any extra-terrestrial caldera. It is also possible to infer some of the eruption characteristics of the extra-terrestrial volcanoes from the morphology of the summit regions, which has implications for the magma supply rate and the input of volatiles into the atmosphere (cf., Robinson et al., 1993 for a discussion of the influence of the eruption of Apollinaris Patera volcano on the Martian atmosphere). The identification of where there has been rapid eruption of lava compared to slow eruptions can be achieved by mapping the distribution of a’*a* (high volumetric flow rate) vs. pahoehoe (low volumetric flow rate) lava flows (Rowland and Walker, 1990). Large areas of Kilauea and Mauna Loa have been covered in the past by tube-fed pahoehoe emanating from an overflowing caldera (Holcomb, 1987;

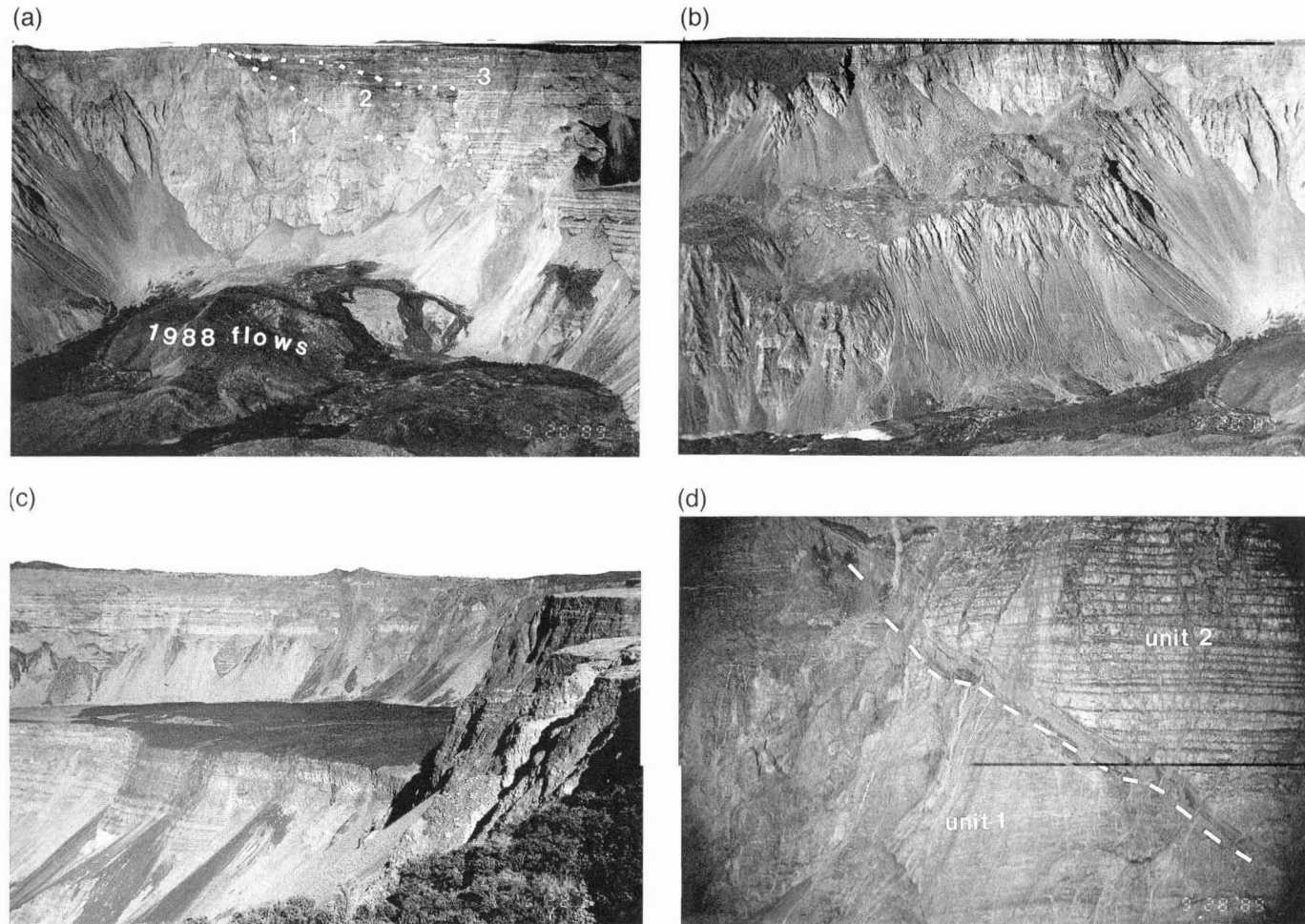


Fig. 18. Ground photographs of the inner wall of Fernandina caldera, Galapagos Islands, obtained in September 1989. (a) The 920 m-high caldera wall has an impressive set of talus fans on both the lower and middle levels. The bright deposits on the floor are playa deposits formed as a result of the engulfment of a summit lake during the September 1988 eruption. Also marked are the unit boundaries shown in (d). From Rowland and Munro (1992). Estimated frame width is  $\sim 2.5$  km. (b) Close-up view of the talus slopes on the eastern wall of Fernandina caldera. The lower set of deposits are estimated to be  $\sim 400$  m high, and have a fluted texture. From the degree of erosion, it appears that these lower deposits are older than the talus fans shown at top left in this view. Estimated frame width is  $\sim 1.5$  km. (c) View of the SE bench. Note the covering of young lavas and the dark talus formed where they spilled over the inboard edge of the bench. Estimated frame width is  $\sim 2$  km. (d) Close-up view of the southern wall, showing two units of flat-lying lava flows (see (a) for location). Unit 1 comprises relatively thin flows, while unit 2 are thick (estimated to be a maximum of  $\sim 10$  m thick). Estimated frame width is  $\sim 0.5$  km.

Lockwood and Lipman, 1987). Tube-fed pahoehoe is very rare on the young Galapagos shields (e.g., Simkin, 1984), and this has been attributed in part to their inability to develop efficient flank conduits (Munro and Rowland, 1993; Rowland et al., 1994).

We can apply the same set of criteria for the volumetric flow rate of lavas to examples on Venus. Due to its low radar backscatter, pahoehoe lava has a lower radar brightness than does a lava at the incidence angles employed by the Magellan spacecraft (Campbell and Campbell, 1992). Thus, in a qualitative manner, the distribution of low and high radar returns at appropriate incidence angles from flow units on Venusian volcanoes is an indication of where low and high volumetric flow rate eruptions have occurred, respectively. Magellan data for Sif Mons, Venus (Fig. 17) shows that radar-dark (low effusion rate?) eruptions have occurred both on the lower flanks and close to the summit on the western side of the volcano. Neither of these areas correlate with the chains of collapse pits, so that the vent systems for these flows must be separate from any hypothesized “rift zone”.

With the exception of calderas on Earth, there seems to have been little intra-caldera activity after the initial period of activity that formed the ponded lavas across the entire caldera floor, as documented for Olympus Mons (Mars) by Mouginis-Mark and Robinson (1992). Despite protracted episodes of caldera collapse, only a few relatively small-volume flows appear to have been erupted within calderas on Mars, although Apollinaris Patera (Mars) is a possible exception (Robinson et al., 1993). On Venus, there are also a few small flows within the caldera of Maat Mons (Fig. 7), but none can be identified within the caldera of Sif Mons (Fig. 14), so that it is not clear what role small-volume intra-caldera eruptions play on Venus after the main collapse episodes. However, the lack of deformation of the smooth floors indicates that at least one episode of flooding by lava took place at both Maat and Sif Montes. One further implication of the analysis of calderas and the distribution of flank vents on Venus is that our observations permit some of the theoretical predictions of Head and Wilson (1992) to be tested. Interestingly, although the summit of Maat Mons is 6 km higher than Sif Mons (8 vs. 2 km above the mean planetary radius), the two summit areas are remark-

ably similar in terms of size, complexity, and the radial distribution of collapse pits. The concept of neutral buoyancy zones on Venus (Head and Wilson, 1992) does not therefore appear to be supported by the landforms found on these two volcanoes.

Although good progress has been made in the interpretation of extra-terrestrial calderas from Viking Orbiter and Magellan images, these data do not permit all aspects of the evolution of the volcanoes to be determined. New types of spacecraft observations, either from orbit or from small landers (such as the Mars Global Surveyor and Mars Pathfinder spacecraft) also need to be made. Improvements in orbital observations would include high spatial resolution ( $< \sim 50$  m/pixel) multi-spectral mapping for Mars, so that different flow units both on the flanks of the volcano and within the exposed caldera walls could be better differentiated. Higher resolution topographic data ( $\sim 100$ – $200$  m spatial resolution) would also help in the analysis of both Martian and Venusian calderas, particularly with respect to the determination of caldera volumes and the slopes of different segments of the caldera floor. Detailed observations of which floor segments have subsided after emplacement might be particularly instructive when considered in conjunction with the morphology of landforms seen on these volcanoes. In the case of Mars, these topographic data will be obtained from a laser altimeter on the Mars Global Surveyor spacecraft, while for Venus an interferometric radar comparable to the type that has already been used for the Earth (Zebker and Goldstein, 1986) would generate topographic information that is more than an order of magnitude better than the data that currently exist. Better gravity data, as well as compositional maps, will have to be obtained from spacecraft yet to be designed, but it is expected that they too would greatly help in the analysis of planetary calderas.

### Acknowledgements

We thank Harold Garbeil, Michelle Tatsumura and Jennifer Parker for the help in the preparation of the figures, Jim Zimelman and Goro Komatsu for reviews, and Vic Baker for his tenacity as Guest Editor for this issue. This work was supported by NASA Grants NAGW-1162 (Geology Program),

NAGW-3500 (Venus Data Analysis Program), and NAGW-437 (Planetary Geology and Geophysics Program). This is HIGP paper no. 1127 and SoEST Publication no. 5311.

## References

- Basaltic Volcanism Study Project, 1981. Basaltic Volcanism on the Terrestrial Planets. Pergamon, New York, 1286 pp.
- Campbell, B.A., Campbell, D.B., 1992. Analysis of volcanic surface morphology on Venus from comparison of Arecibo, Magellan, and terrestrial airborne radar data. *J. Geophys. Res.*, 97, 16293–16314.
- Carr, M.H., 1973. Volcanism on Mars. *J. Geophys. Res.*, 78, 4049–4062.
- Carr, M.H., Greeley, R., Blasius, K.R., Guest, J.E., Murray, J.B., 1977. Some Martian volcanic features as viewed from the Viking Orbiters. *J. Geophys. Res.*, 82, 3985–4015.
- Cattermole, P., 1986. Linear volcanic features at Alba Patera, Mars—probable spatter ridges. *J. Geophys. Res.*, 91, E165–E1959.
- Cattermole, P., 1990. Volcanic flow development at Alba Patera, Mars. *Icarus*, 83, 453–493.
- Chadwick, W.W., Howard, K.A., 1991. The pattern of circumferential and radial eruptive fissures on the volcanoes of Fernandina and Isabela islands, Galapagos. *Bull. Volcanol.*, 53, 259–275.
- Chadwick, W.W., De Roy, T., Carrasco, A., 1991. The September 1988 intracaldera avalanche and eruption at Fernandina volcano, Galapagos Islands. *Bull. Volcanol.*, 53, 276–286.
- Decker, R.W., 1987. Dynamics of Hawaiian volcanoes: an overview. Volcanism in Hawaii. U.S. Geol. Surv. Prof. Pap., vol. 1350, pp. 997–1018.
- Delaney, J.R., Colony, W.E., Gerlach, T.M., Nordlie, B.E., 1973. Geology of the Volcan Chico area on Sierra Negra volcano, Galapagos Islands. *Geol. Soc. Am. Bull.*, 84, 2455–2470.
- Delaney, P.T., Fiske, R.S., Miklius, A., Okamura, A.T., Sato, M.K., 1990. Deep magma body beneath the summit and rift zones of Kilauea volcano, Hawaii. *Science*, 247, 1311–1316.
- Devorak, J.J., 1992. Mechanism of explosive eruptions of Kilauea volcano, Hawaii. *Bull. Volcanol.*, 54, 638–645.
- Fiske, R.S., Kinoshita, W.T., 1969. Inflation of Kilauea volcano prior to its 1967–1968 eruption. *Science*, 165, 341–349.
- Francis, P.W., 1993. Volcanoes: A Planetary Perspective. Oxford Univ. Press, New York, NY, 443 pp.
- Grimm, R.E., Phillips, R.J., 1992. Anatomy of a Venusian hot spot: geology, gravity, and mantle dynamics of Eistla Regio. *J. Geophys. Res.*, 97, 16035–16054.
- Head, J.W., Wilson, L., 1992. Magma reservoirs and neutral buoyancy zones on Venus: implications for the formation and evolution of volcanic landforms. *J. Geophys. Res.*, 97, 3877–3903.
- Head, J.W., Crumpler, L.S., Aubele, J.C., Guest, J.E., Saunders, R.S., 1992. Venus volcanism: classification of volcanic features and structures, associations, and global distribution from Magellan data. *J. Geophys. Res.*, 97, 13153–13197.
- Heliker, C., Wright, T.L., 1991. The Pu'u 'O'o Kupaianaha eruption of Kilauea. *Eos* 72, 521, 526, 530.
- Holcomb, R.T., 1987. Eruptive history and long-term behavior of Kilauea volcano. Volcanism in Hawaii. U.S. Geol. Surv. Prof. Pap., vol. 1350, pp. 261–350.
- Ivanov, M.A., Basilevsky, A.T., 1990. Coronae and major shields on Venus: comparison of their areas, basal altitudes and areal distributions. *Earth, Moon, Planets*, 50/51, 409–420.
- Jaggard, T.A., 1947. Origin and development of craters. *Geol. Soc. Am., Mem.*, 21, 508 pp.
- Janle, P., Ropers, J., 1983. Investigation of the isostatic state of the Elysium dome on Mars by gravity models. *Phys. Earth Planet. Inter.*, 32, 132–145.
- Klein, F.W., Koyanagi, R.Y., Nakata, J.S., Tanigawa, W.R., 1987. The seismicity of Kilauea's magma system. U.S. Geol. Surv. Prof. Pap., 1350, 1019–1185.
- Koyanagi, R.Y., Swanson, D.A., Endo, E.T., 1972. Distribution of earthquakes related to mobility of the south flank of Kilauea volcano, Hawaii. U.S. Geol. Surv. Prof. Pap., 800-D, 89–97.
- Lipman, P.W., 1980a. The southwest rift zone of Mauna Loa—implications for structural evolution of Hawaiian volcanoes. *Am. J. Sci.*, 280-A, 752–776.
- Lipman, P.W., 1980b. Rates of volcanic activity along the southwest rift zone of Mauna Loa volcano. *Bull. Volcanol.*, 43, 703–725.
- Lockwood, J.P., Lipman, P.W., 1987. Holocene eruptive history of Mauna Loa volcano. Volcanism in Hawaii. U.S. Geol. Surv. Prof. Pap., vol. 1350, pp. 509–535.
- Macdonald, G.A., 1965. Hawaiian calderas. *Pac. Sci.*, 19, 320–334.
- Macdonald, G.A., 1972. Volcanoes. Prentice-Hall, Englewood Cliffs, NJ, 510 pp.
- Macdonald, G.A., Abbott, A.T., Peterson, F.L., 1983. Volcanoes in the Sea: The Geology of Hawaii. Univ. Hawaii Press, Honolulu, 517 pp.
- Malin, M.C., 1977. Comparison of volcanic features of Elysium (Mars) and Tibesti (Earth). *Geol. Soc. Am. Bull.*, 88, 908–919.
- McBirney, A.R., Williams, H., 1969. Geology and petrology of the Galapagos Islands. *Geol. Soc. Am., Mem.*, 118, 197 pp.
- Miller, T.P., Smith, R.L., 1987. Late Quaternary caldera-forming eruptions in the eastern Aleutian arc, Alaska. *Geology*, 15, 434–438.
- Mougini-Mark, P.J., 1981. Late-stage summit activity of Martian shield volcanoes. *Proc. Lunar Planet. Sci.*, 12B, 1431–1447.
- Mougini-Mark, P.J., Robinson, M.S., 1992. Evolution of the Olympus Mons caldera, Mars. *Bull. Volcanol.*, 54, 347–360.
- Mougini-Mark, P.J., Wilson, L., Zimbelman, J.R., 1988. Polygenic eruptions on Alba Patera, Mars. *Bull. Volcanol.*, 50, 361–379.
- Mougini-Mark, P.J., Wilson, L., Zuber, M.T., 1992. The physical volcanology of Mars. In: Kieffer, H.H., Jakosky, B.M., Snyder, C.W., Matthews, M.S. (Eds.), Mars. Univ. Arizona Press, Tucson, AZ, pp. 424–452.
- Munro, D.C., 1992. The Application of Remotely Sensed Data to Studies of Volcanism Within the Galapagos Islands. Unpublished PhD thesis, University of Hawaii, Honolulu, HI, 306 pp.
- Munro, D.C., Rowland, S.K., 1993. Structural influences on the

- distribution of eruptive vents in the western Galapagos. Abstract Vol. IAVCEI General Assembly (Canberra), p. 77.
- Munro, D.C., Rowland, S.K., Mougini-Mark, P.J., Wilson, L., Oviedo-Perez, V.H., 1991. An investigation of the distribution of eruptive products on the shield volcanoes of the western Galapagos Islands using remotely sensed data. Eighth Thematic Conference on Geologic Remote Sensing, Denver, CO (April 29–May 2, 1991), pp. 1161–1174.
- Nakamura, K., 1977. Volcanoes as possible indicators of tectonic stress orientation—principle and proposal. *J. Volcanol. Geotherm. Res.*, 2, 1–16.
- Nakamura, K., 1982. Why do long rift zones develop better in Hawaiian volcanoes—a possible role of thick sediments. *Bull. Volcanol. Soc. Jpn.*, 25, 225–267.
- Nordlie, B.E., 1973. Morphology and structure of the western Galapagos volcanoes and a model for their origin. *Geol. Soc. Am. Bull.*, 84, 2931–2956.
- Richards, A.F., 1960. Archipelago de Colon, Isla San Felix and Islas Juan Fernandez. *Catalog of Active Volcanoes of the World*, vol. 14, IAVCEI, Rome, 50 pp.
- Robinson, M.S., 1994. Some aspects of lunar and Martian volcanism as examined with spectral, topographic, and morphologic data derived from spacecraft images. Unpub. PhD Thesis, University of Hawaii, Honolulu, HI.
- Robinson, M.S., Mougini-Mark, P.J., Zimbelman, J.R., Wu, S.C., Ablin, K.K., Howington-Kraus, A.E., 1993. Chronology, eruption duration, and atmospheric contribution of the Martian volcano Apollinaris Patera. *Icarus*, 104, 301–323.
- Rowland, S.K., Munro, D.C., 1992. The caldera of Volcan Fernandina: a remote sensing study of its structure and recent activity. *Bull. Volcanol.*, 55, 97–109.
- Rowland, S.K., Walker, G.P.L., 1990. Pahoehoe and a'a in Hawaii: volumetric flow rate controls the lava structure. *Bull. Volcanol.*, 52, 615–628.
- Rowland, S.K., Munro, D.C., Perez-Oviedo, V., 1994. Volcan Ecuador, Galapagos Islands: erosion as a possible mechanism for the generation of steep-sided basaltic volcanoes. *Bull. Volcanol.*, 56, 271–283.
- Ryan, M.P., 1988. The mechanics and three-dimensional internal structure of active magmatic systems: Kilauea, Hawaii. *J. Geophys. Res.*, 93, 4213–4248.
- Schaber, G.G., 1982. Syrtis Major: a low-relief volcanic shield. *J. Geophys. Res.*, 87, 9852–9866.
- Senske, D.A., Schaber, G.G., Stofan, E.R., 1992. Regional topographic rises on Venus: geology of Western Eistla Regio and comparison to Beta Regio and Atla Regio. *J. Geophys. Res.*, 97, 13395–13420.
- Simkin, T., 1984. The geology of the Galapagos Islands. In: Perry, R. (Ed.), *Galapagos*. Pergamon, Oxford, pp. 15–41.
- Simkin, T., Howard, K.A., 1970. Caldera collapse in the Galapagos Islands. *Science*, 169, 429–437.
- Strong, D.F., Jaquot, C., 1971. The Karthala caldera, Grand Comore. *Bull. Volcanol.*, 34, 663–680.
- Swanson, D.A., Duffield, W.A., Jackson, D.B., Peterson, D.W., 1979. Chronological narrative of the 1969–1971 Mauna Ulu eruption of Kilauea volcano, Hawaii. *U.S. Geol. Surv. Prof. Pap.*, 1056, 55 pp.
- Tilling, R.I., Christianson, R.L., Duffield, W.A., Endo, E.T., Holcomb, R.T., Koyanagi, R.Y., Peterson, D.W., Unger, J.D., 1987. The 1972–1974 Mauna Ulu eruption, Kilauea volcano: an example of quasi-steady-state magma transfer. *U.S. Geol. Surv. Prof. Pap.*, 1350, 405–469.
- Upton, B.J.G., Wadsworth, W.J., Latrille, E., 1974. The 1972 eruption of Karthala (sic) Volcano, Grande Comoro. *Bull. Volcanol.*, 38, 136–148.
- Walker, G.P.L., 1988. Three Hawaiian calderas: origin through loading by shallow intrusions? *J. Geophys. Res.*, 93, 14773–14784.
- Williams, H., McBirney, A.R., 1979. *Volcanology*. Freeman, San Francisco, CA, 379 pp.
- Wilson, C.J.N., Rogan, A.M., Smith, I.E.M., Northey, D.J., Nairn, I.A., Houghton, B.F., 1984. Caldera volcanoes of the Taupo volcanic zone, New Zealand. *J. Geophys. Res.*, 89, 8463–8484.
- Wilson, L., Head, J.W., 1983. A comparison of volcanic eruption processes on Earth, Moon, Mars, Io and Venus. *Nature*, 302, 663–669.
- Wood, C.A., 1984. Calderas: a planetary perspective. *J. Geophys. Res.*, 89, 8391–8406.
- Zebker, H.A., Goldstein, R.M., 1986. Topographic mapping derived from synthetic aperture radar measurements. *J. Geophys. Res.*, 91, 4993–4999.
- Zimbelman, J.R., Edgett, K.S., 1992. The Tharsis Montes, Mars: comparison of volcanic and modified landforms. *Proc. Lunar Planet. Sci.*, 22, 31–44.
- Zuber, M.T., Mougini-Mark, P.J., 1992. Caldera subsidence and magma chamber depth of the Olympus Mons volcano, Mars. *J. Geophys. Res.*, 97, 18295–18307.